Title

Distinctive features of the D101N and D101G variants of superoxide dismutase 1; two mutations that produce rapidly progressing motor neuron disease.

Journal

Journal of neurochemistry, 128(2)

ISSN

0022-3042

Authors

Ayers, Jacob
Lelie, Herman
Workman, Aron
et al.

Publication Date

2014

DOI

10.1111/jnc.12451

Peer reviewed

Published in final edited form as:
J Neurochem. 2014 January ; 128(2): 305–314. doi:10.1111/jnc.12451.

Distinctive features of the D101N and D101G variants of superoxide dismutase 1; two mutations that produce rapidly progressing motor neuron disease

Jacob Ayers[1,*], **Herman Lelie**[3,*], **Aron Workman**[1,*], **Mercedes Prudencio**[2,*], **Hilda Brown**[1], **Susan Fromholt**[1], **Joan Valentine**[3], **Julian Whitelegge**[4], and **David Borchelt**[1,†]

[1]Department of Neuroscience, Center for Translational Research in Neurodegenerative Disease, McKnight Brain Institute, University of Florida, Gainesville, Florida 32610

[2]Department of Neuroscience, Mayo Clinic Jacksonville, 4500 San Pablo Rd S, Jacksonville, FL, 32224

[3]Department of Chemistry and Biochemistry, UCLA, Los Angeles, California 90095

[4]The Pasarow Mass Spectrometry Laboratory, NPI-Semel Institute, David Geffen School of Medicine, UCLA, Los Angeles, California 90024

Abstract

Mutations in superoxide dismutase 1 (SOD1) associated with familial amyotrophic lateral sclerosis (fALS) induce misfolding and aggregation of the protein with the inherent propensity of mutant SOD1 to aggregate generally correlating, with a few exceptions, to the duration of illness in patients with the same mutation. One notable exception was the D101N variant, which has been described as wild-type-like. The D101N mutation is associated with rapidly progressing motor neuron degeneration but shows a low propensity to aggregate. By assaying the kinetics of aggregation in a well characterized cultured cell model, we show that the D101N mutant is slower to initiate aggregation than the D101G mutant. In this cell system of protein over-expression, both mutants were equally less able to acquire Zn than WT SOD1. Additionally, both of these mutants were equivalently less able to fold into the trypsin-resistant conformation that characterizes WT SOD1. A second major difference between the two mutants was that the D101N variant more efficiently formed a normal intramolecular disulfide bond. Overall, our findings demonstrate that the D101N and D101G variants exhibit clearly distinctive features, including a different rate of aggregation, and yet both are associated with rapidly progressing disease.

Keywords

ALS; SOD1; aggregation; oxidation; stability

Introduction

Amyotrophic lateral sclerosis (ALS) is a fatal neurodegenerative disease that selectively targets motor neurons. Although the majority of cases are sporadic (sALS) in nature, around 5% of cases are familial (fALS) and have a genetically inherited component. Mutations in

†To whom correspondence should be addressed: David Borchelt, Department of Neuroscience/CTRND, Box 100159, University of Florida, Gainesville, FL 32610, USA, Tel.: (352) 273-9664; borchelt@mbi.ufl.edu; drb1@ufl.edu.
*These authors contributed equally to this work.

The authors declare that they have no competing interests.

the *SOD1* gene, which codes for the ubiquitously expressed homodimeric metalloenzyme SOD1, are known to be causative in 10–20% of fALS cases. To date, there have been 165 SOD1 mutations described in either familial or, less frequently, sporadic ALS cases (http://alsod.iop.kcl.ac.uk). Interestingly, the duration of disease (from less than 2 years to more than 10) varies in a nonrandom fashion among patients such that some mutations are associated with disease of short duration whereas others are associated with disease of long duration (Cudkowicz *et al.* 1997, Prudencio *et al.* 2009b).

Although it was first unclear whether toxicity in SOD1-mediated fALS disease was due to a loss of enzymatic function, it is now accepted that mutated SOD1 results in the acquisition of toxic properties (Borchelt *et al.* 1995, Borchelt *et al.* 1994). The SOD1 protein is subject to several post-translational modifications including the insertion of copper (Cu) and zinc (Zn) ions, the formation of a disulfide bond, and dimerization (Doucette *et al.* 2004, Potter *et al.* 2007). Many fALS-linked SOD1 mutants can achieve enzymatically active conformations that exhibit biophysical profiles indistinguishable from the wild-type protein (Borchelt et al. 1995, Borchelt et al. 1994, Rodriguez *et al.* 2005). However, multiple studies have demonstrated that mutation-induced conformational changes of the protein lead to misfolding that manifests as the formation of detergent-insoluble protein aggregates; these aggregates have been observed both in patients and transgenic mouse models expressing mutant SOD1 (Bruijn *et al.* 1998, Karch *et al.* 2009, Prudencio et al. 2009b, Wang *et al.* 2003, Watanabe *et al.* 2001). The formation of SOD1 aggregates has also been reliably demonstrated in cultured cells, which have proven to be a valuable tool in studying the variability in mutant SOD1 aggregation (Prudencio & Borchelt 2011, Prudencio et al. 2009b, Wang et al. 2003).

In studies investigating the propensity of a number of SOD1 mutants to aggregate we demonstrated that there was an inverse relationship between high-aggregation propensity and the duration of disease in SOD1-fALS patients; the majority of mutants associated with rapidly progressing disease exhibited high propensities to aggregate (Prudencio et al. 2009b). However, several mutants associated with a rapid disease course exhibited a low propensity to aggregate. One of these mutants was the D101N variant; a site that can also be mutated to D101G in ALS patients. Both of these mutations are associated with rapidly progressing disease (2.4 years; n=14 patients with D101N and n=3 patients with D101G) (Prudencio et al. 2009b). The D101N variant of SOD1 can be isolated in a state that exhibits a similar tertiary structure, activity, Zn metallation state, and stability to WT SOD1 (Bystrom *et al.* 2010, Chattopadhyay & Valentine 2009, Rodriguez et al. 2005, Prudencio et al. 2009b). In comparison, the D101G variant markedly destabilizes the protein (Bystrom et al. 2010, Prudencio et al. 2009b). Thus, although the D101N and D101G mutations both produce a decrease in the negative charge of SOD1, these proteins exhibit divergent biophysical characteristics. In the present study, we sought to determine the basis for the different aggregation propensities of these two mutants using a previously characterized HEK293FT cell culture model (Karch & Borchelt 2008, Karch et al. 2009, Prudencio & Borchelt 2011, Prudencio *et al.* 2009a, Prudencio *et al.* 2010, Prudencio et al. 2009b, Prudencio *et al.* 2012). Our data demonstrate that as compared to the D101G variant, the D101N variant of SOD1 exhibits a longer lag phase to initiate aggregation. In this over-expression model, neither protein efficiently acquired Cu, or Zn, and both failed to fold into trypsin-resistant conformations. A second major biophysical difference between the two mutants was that the D101N variant more efficiently formed the normal intramolecular disulfide bond. Our data demonstrate that variants with substantially different characteristics can cause rapidly progressing forms of ALS.

Methods

Tissue culture transfection and pulse-chase labeling

SOD1 constructs (4ug) were transfected into HEK293FT cells using Lipofectamine 2000 (Invitrogen, Carlsbad, CA, USA), for 24 or 48 hours, as indicated in the figure legends, at 37°C with 5% CO_2. After 3–5 hours, complete media (DMEM with 10% horse serum and 2mM L-glutamine) was added to the cells. For pulse-chase labeling, at 24 hours post-transfection, cells were rinsed with DPBS, then incubated in cysteine-free media for 1 hour. This was followed by incubating the cells in ^{35}S-Cysteine media (300 uCi/ml) for 1 hour at 37°C. Cells were then either harvested following this 1 hour incubation or harvested after an additional incubation for 24 hours at 37°C with 5% CO_2 in cysteine-free media.

Detergent extraction, immunopurification, and visualization of radiolabeled SOD1 protein

The cells were either washed 3 times in DPBS then scraped off the bottom of the dish or collected by aspiration of the media and washed 3 times in DPBS by repeated centrifugation and resuspension. Cells were then centrifuged at low speed (~800 × g) for 10 minutes and resuspended in 1X TEN buffer (10 mM Tris, pH 7.5; 1 mM EDTA, pH 8.0; 100 mM NaCl) containing 1:100 v/v protease inhibitor cocktail (Sigma, St. Louis, MO, USA) and 0.5% NP-40. The cells were then lysed by sonicating the samples two times for 15 seconds each before centrifugation at >100,000 × g for 5 minutes in a Beckman AirFuge (Brea, CA, USA) to produce supernatant 1 (S1) and pellet (P1) fractions. The S1 fractions were put on ice, and the P1 fractions were washed with the same extraction buffer, sonicated and centrifuged as before. The supernatant was discarded and the remaining pellet (P2) was resuspended by sonication in 1X TEN buffer containing 0.5% NP-40, 0.25% SDS, 0.5% deoxycholate, and 1:100 v/v protease inhibitor cocktail.

SDS and deoxycholate were added to the S1 samples to 0.25% and 0.5% respectively. Samples were then boiled for 10 minutes, cooled at room temperature, and spun at 16,000xg for 5 minutes. The supernatant was collected and cooled on ice for 5 minutes. A rabbit SOD-1 antibody was added at 1:100 to the S1 and P2 samples and incubated overnight at 4°C with shaking. 50ul of Protein A agarose (Pierce Biotechnology, Rockford, IL, USA) was then added to the samples and gently shaken for 1.5 – 2 hours at room temperature. After the samples were spun at 3000×g for 3 minutes, the supernatant was removed and the agarose beads were washed with 500ul of the 1X TEN buffer containing SDS and deoxycholate for 30 minutes at 4°C with shaking. The samples were then spun again at 3000×g for 3 minutes and this wash procedure was repeated an additional 3 times. During the last wash, the beads were transferred to a clean tube, and then pelleted by centrifugation. The supernatant was removed and the beads were resuspended in 30ul of 2X Laemmli buffer, boiled for 5 minutes in Laemmli sample buffer and electrophoresed in 18% Tris-Glycine gels (Invitrogen, Carlsbad, CA, USA). The gel was then soaked in Amplify (GE Healthcare, Pittsburgh, PA, USA), dried, and exposed to film.

Detergent extraction and trypsin digestion of SOD1 for disulfide bond analysis

Following a 24 hour transfection, cells were scraped from the dish in DPBS and washed 3 times in DPBS by repeated centrifugation and resuspension. After the final wash, cells were resuspended by sonication three times for 10 seconds each in 1X TEN buffer containing 1% NP-40, 200mM iodoacetamide, and 1:100 v/v protease inhibitor cocktail before centrifugation at >100,000 × g for 5 min in an AirFuge to produce supernatant 1 (S1) and pellet (P1) fractions. The S1 fractions were put on ice, and the P1 fractions were washed with the same extraction buffer, sonicated three times for 10 seconds each, and centrifuged at >100,000 × g for 5 min. The supernatant was discarded and the remaining pellet (P2) was resuspended by pulsed sonication in 1X TEN buffer containing 0.5% NP-40, 100mM

iodoacetamide, and protease inhibitors. The protein concentrations of the S1 and P2 fractions were then determined by BCA assay, as described by the manufacturer (Pierce Biotechnology, Rockford, IL, USA). For trypsin digests, the protease inhibitor cocktail was omitted from all buffers. For digestion, 5 μg of the S1 fraction and 20 μg of the P2 fraction were incubated with trypsin at final concentrations of 0, 10, and 100 μg/ml for 30 minutes at 37°C. Digestions were stopped by the addition of Laemmli sample buffer and immediately boiling the sample at 100°C.

Western blot analysis

5 μg of the S1 fractions and 20 μg of the P2 fractions were boiled for 5 minutes in Laemmli sample buffer with β-mercaptoethanol (βME), or without for non-reducing SDS-PAGE, and electrophoresed in 18% Tris-Glycine gels (Invitrogen, Carlsbad, CA, USA). For non-reducing SDS-PAGE, an in-gel reduction was accomplished by incubating gels in transfer buffer with 2% βME for 10 minutes prior to transferring to nitrocellulose membrane. Following transfer, membranes were blocked in 5% milk in PBS-T (1X PBS, 0.1% Tween-20) for 30 minutes then incubated for 1 hour at room temperature or overnight at 4°C with the rabbit polyclonal antibodies m/h SOD (Borchelt et al. 1994) or hSOD (Bruijn et al. 1998) at 1:2500 in PBS-T and 5% milk. The membrane was then washed with PBS-T, incubated for 1 hour at room temperature with a goat anti-rabbit secondary antibody at 1:5000 in PBS-T and 5% milk before developing with ECL reagents (Thermo Scientific Inc., Rockford, IL, USA) and visualizing with a Fujifilm imaging system (FUJIFILM Life Science, Stamford, CT, USA). The aggregation propensity was assessed by comparing the ratio of immunoreactive SOD1 bands in the P2 versus S1 fractions as previously described (Prudencio et al. 2009a).

SOD1 metal-binding characterization

The level of Cu and Zn bound to soluble SOD1 isolated from cultured cells, which had been transfected for 24 hours, was determined using methods previously described (Lelie *et al.* 2011, Prudencio et al. 2012). Briefly, 40ul of the NP-40 detergent soluble supernatants (S1) from transfected cells were loaded onto an Agilent 1200 series HPLC size exclusion column (SWX 2000 TOSOH Biosciences; resolvable range 5 kDa to 150 kDa), and the proteins were segregated using a 30 minute isocratic gradient with a trace element free mobile phase (25mM potassium phosphate pH 6.7, 25 mM sodium chloride). The absorbance at 214 was used to monitor SOD1 peak elution and measure the protein concentration. The eluent directly flowed in-line into the ICP-MS where Cu, Zn, manganese, and iron concentrations were then measured in real-time allowing for accurate Cu and Zn concentration from the SOD1 peak. SOD1 metallation was determined by dividing SOD1 metal concentration by the SOD1 protein concentration.

Statistical analyses

All statistical analyses were analyzed in GraphPad PRISM 5.01 Software (La Jolla, CA) as explained in figure legends.

RESULTS

Kinetics of insoluble aggregate formation in HEK293FT cells expressing mutant SOD1

When overexpressed in HEK293FT cells, the D101G mutant of SOD1 produces much larger amounts of detergent insoluble aggregates at both 24 and 48 hours post-transfection than the D101N mutant (Prudencio et al. 2009b). To allow a side-by-side comparison, we transiently transfected HEK293FT cells for 48 hours with WT SOD1 and the mutants, A4V, D101G, and D101N. Although the D101N mutant accumulated a significant amount of insoluble

SOD1 when compared to WT SOD1, the amount of insoluble D101G and A4V SOD1 was much greater (Fig. 1*A* and *B*). To determine how the kinetics of aggregation differ between the D101N and D101G mutants, HEK293FT cells were transiently transfected and cells were harvested at defined intervals post-transfection followed by detergent extraction and analysis by immunoblot. Detectable levels of insoluble SOD1 first appeared for D101G at 12 hours following transfection and rose steadily over 48 hours post-transfection. Whereas insoluble D101N was not detected until 24 hours the accumulated robustly over the next 24 hours (Fig. 1*C* and *D*; Fig. S1). Together these data suggested that the low propensity of the D101N variant of SOD1 to aggregate in 24 or 48 hour intervals is due to a to a longer lag phase to initiate aggregation.

To further examine the kinetics of mutant SOD1 aggregation of these two mutants, we used pulse-chase labeling of SOD1 following a transient transfection in HEK293FT cells. Because the only methionine in SOD1 is the initiator start site and because this methionine is lost by post-translational N-terminal acetylation (Borchelt *et al.* 1998), radiolabeled methionine cannot be used to metabolically radiolabel SOD1. Following a previously established protocol for metabolic labeling with pulse-chase, we used radiolabeled cysteine for these studies (Borchelt et al. 1998). Radiolabeled cysteine is the only other sulfur containing amino acid that allows for the use of more energetic isotopes. For this experiment, we used a paradigm in which the cells were pulse-labeled for 1 hour at 24 hours post-transfection. At this time point, cells expressing the D101G variant appear to be exponentially increasing the levels of misfolded SOD1 (Fig. 1D) and we observed that a significant amount of mutant SOD1 labeled in the 1 hour pulse partitioned into the detergent-insoluble fraction (Fig. 1*E* and *F*). Conversely, at 24 hours post-transfection cells expressing the D101N mutant have not yet shown evidence of accumulation of insoluble protein (Fig 1D) and very little of the newly labeled protein partitioned into the detergent-insoluble fraction (Fig. 1*E* and *F*). However, following a 24 hour chase in unlabeled media (or 48 hours post-transfection), approximately 60% of the radiolabeled D101N mutant had become detergent-insoluble. In the case of the D101G mutant, the percentage of newly made protein that became detergent-insoluble during the pulse label was somewhat lower (~50%) and the overall level of radiolabeled D101G protein that was detergent insoluble at 48 hours was less than that of the D101N mutant; suggesting that some of the D101N mutant protein that acquired detergent-insolubility at 1 hour either became soluble or was degraded. Importantly, the level of radiolabeled D101N SOD1 that was immunoprecipitated in a 1 hour pulse was similar to that of D101G SOD1, indicating that the basal level of expression of mutant SOD1 between the two cultures was not significantly different. We also noted that the level of labeled D101G protein in the soluble fraction decreased at 48 hours, and coupled with a lack of appearance of this labeled protein in the insoluble fraction we assume that the mutant SOD1 that did not assemble into more stable aggregates was degraded.

Analysis of intramolecular disulfide bond formation and metallation

The differences in aggregation rates between the D101N and D101G mutants could be due to differences in acquisition of post-translational modifications to the protein. Previous studies have demonstrated that different mutations associated with ALS produced varied effects on the formation of intramolecular disulfide bonds between cysteines 57 and 146 (Karch et al. 2009). To examine the formation of this bond in the D101G and D101N mutants, in comparison to WT SOD1, in our cell model of aggregation, we assessed the migration rates of these SOD1 proteins in non-reducing SDS/PAGE; using in-gel reduction to enhance the detection of the oxidized SOD1 by immunoblot analysis (Zetterstrom *et al.* 2007). In the soluble fractions at 24 hours post-transfection, less than a third of the WT SOD1 protein had acquired a disulfide bond, whereas by 48 hours the ratio of oxidized to reduced SOD1 was ~ 1:1 (Fig. 2). In comparison, at either 24 or 48 hours, the vast majority

of the detergent-soluble D101G SOD1 remained reduced. The D101N SOD1 mutant, however, produced a pattern more similar to WT SOD1, with a greater percentage of the protein acquiring a disulfide bond by 48 hours (Fig. 2). These data reveal that, in the context of these cell expression models, the D101N variant is significantly more efficient in acquiring the normal intramolecular disulfide bond than the D101G variant.

Since the binding of Cu and Zn to SOD1 has been previously shown to increase the structural stability of the protein, which could influence aggregation rates, we investigated the binding of Cu and Zn to SOD1 in our cell model. We have previously demonstrated that when overexpressed in cell culture, WT SOD1 shows a reduced incorporation of Cu (Prudencio et al. 2012). Even though we could detect incorporated Cu in endogenous SOD1 from untransfected HEK293FT cells, we were unable to detect any Cu bound to the overexpressed WT or mutant SOD1 in our transfected cells (Fig. 3). By contrast, the levels of Zn incorporated into overexpressed WT SOD1 were near normal, while both the D101G and D101N SOD1 mutants showed much poorer incorporation of Zn in this system (Fig. 3).

Assessment of WT and mutant SOD1 folding by sensitivity to trypsin digestion

WT SOD1 is a hyperstable protein that shows extreme proteolytic resistance, whereas mutant SOD1 variants exhibit variable sensitivities to proteolytic digestion (Ratovitski *et al.* 1999). To determine how overexpression of SOD1 in our cell culture model of aggregation impacted folding, we examined the sensitivity of WT and mutant SOD1 to trypsin digestion. For this study, we assessed the protease sensitivity of SOD1 in NP-40 detergent-soluble and insoluble fractions and analyzed these fractions by non-reducing SDS/PAGE to determine whether oxidized and reduced forms of the proteins displayed different sensitivities to trypsin digestion. Importantly, despite the low incorporation of Cu and the slowness of disulfide formation in this cell model, WT SOD1, which was found only in the NP40 soluble fractions, displayed the expected extreme resistance to trypsin digestion (Fig. 4*A* and *B*). Both reduced and oxidized fractions of soluble WT SOD1 displayed similar levels of resistance to proteolytic digestion (Fig. 4*A* and *B*). For mutant D101G and D101N SOD1 that fractionated into the NP40 soluble fraction, protein lacking a disulfide bond displayed high sensitivity to proteolysis, whereas the oxidized protein displayed slightly greater resistance (Fig. *A* and *C–D*).

Previous studies have established that the normal disulfide bond of the detergent-insoluble forms of mutant SOD1 is reduced; and that disulfide cross-links between mutant proteins produce multiple bands on SDS-PAGE (Furukawa *et al.* 2008, Karch et al. 2009, Zetterstrom et al. 2007). Thus, for analysis of the P2 fraction, we analyzed the proteins that survive trypsin digestion by immunoblotting standard SDS-PAGE with reducing agents so that we would have a single band to quantify. As compared to reduced or oxidized, soluble WT SOD1, the insoluble D101G and D101N variants displayed higher sensitivity to trypsin digestion. Insoluble mutant SOD1 proteins were completely degraded by 100 μg/ml trypsin in 30 min at 37°C (Fig. 5), whereas oxidized WT SOD1 is completely resistant and ~50% of reduced soluble WT SOD1 survives this condition (see Fig. 4). However, we noted that as compared to soluble forms of D101G or D101N SOD1, the insoluble proteins were significantly more resistant to trypsin (resisting digestion by 10 μg/ml of trypsin for 30 minutes at 37°C) (Fig. 5). Overall, these findings indicate that both soluble and insoluble forms of D101N and D101G proteins fail to achieve native conformations when overexpressed in HEK293FT cells. The data further indicate that the conformation of detergent-insoluble D101N and D101G proteins differ from that of the soluble forms.

DISCUSSION

In multiple prior studies, we found that overexpression of mutant SOD1 in HEK293FT cells is a valuable system for assessing the impact of ALS associated mutations on the aggregation propensity of SOD1 (Karch et al. 2009, Prudencio et al. 2009b, Prudencio et al. 2012). In this system, the overexpression of SOD1 overwhelms most cellular systems associated with protein homeostasis and post-translational regulation and reveals inherent properties of mutant SOD1. In a prior study of the aggregation propensity of the D101N and D101G variants of SOD1 in this system, we found that cells expressing the D101N variant accumulate less misfolded aggregates of mutant SOD1 than cells expressing the D101G variant (Prudencio et al. 2009b). In the present study, we have used this same cell culture system to further examine the aggregation of these variants and define the properties that may account for different aggregation propensities (Table 1). In studies of aggregation kinetics, we determined that the D101N variant displays a longer lag phase before the initial appearance of insoluble protein as compared to the D101G variant; suggesting that the nucleation of aggregation by D101N is slower than that of the D101G variant. However, once aggregation initiated, the relative efficiencies with which newly made D101N protein that acquired the detergent-insoluble conformation was similar to that of the D101G mutant. As compared to WT SOD1 expressed at similar levels, our findings indicate that both of these mutations significantly impact the post-translational modification and structural stability of SOD1. Although the D101N variant was similar to WT SOD1 in efficiency to form an intramolecular disulfide bond, the D101N variant was much less able to bind zinc than WT SOD1 and showed a much higher sensitivity to trypsin digestion than the WT protein. The D101G variant appeared to be slightly more severely affected, as this mutant was less able to form intramolecular disulfide bonds on top of its inability to bind Zn or acquire trypsin-resistant conformations.

Although the role of large aggregates of mutant SOD1 in the pathogenesis of motor neuron disease is uncertain, it is clear that the propensity to aggregate is a reflection of misfolding and that, in transgenic mouse models, disease is always associated with an accumulation of aggregates of mutant SOD1; mice expressing the mutant protein at levels too low to cause disease do not develop aggregates of mutant SOD1(Deng *et al.* 2006, Jaarsma *et al.* 2000, Wang *et al.* 2005). Thus, aggregation seems to be linked to toxicity in some manner.

As stated in the Introduction, both the D101G and D101N mutants are associated with rather short disease durations of about 2.5 years. Previously, we had thought the short disease duration period of the D101N variant was discordant with its apparent aggregation propensity because the general trend we observed across a large number of mutants was that mutations associated with faster rates of progression showed high propensities to aggregate (Prudencio et al. 2009b). In the present study, we show that the low apparent propensity of the D101N mutant to aggregate, as measured in this cell system, is due to a longer lag phase to initiate aggregate formation. If we associate aggregation with toxicity, then we would presume that the lag phase to initiation of aggregation should be a modulator of onset whereas the rate with which soluble precursor converts to insoluble aggregate should be a modulator of duration. Our pulse-chase studies of aggregation demonstrate that once aggregation initiated the percent of newly made D101N protein that acquired a detergent insoluble conformation was similar to that of the D101G mutant. Thus, the apparent discordance between overall aggregation propensity of the D101N and D101G variants and disease duration may be resolved by relating disease duration to the relative efficiency by which soluble mutant SOD1 acquires insoluble conformations once aggregation has initiated. Additional studies of a larger set of mutants that includes mutants associated with slowly progressing disease are required to determine whether this proposed relationship

holds. The current picture is one in which we have two variants that alter a single position with clearly distinguishable properties that produce disease of short duration.

Both the D101N and D101G mutants contain amino acid substitutions that eliminate a negatively charged residue (aspartate), which has been suggested as potentially contributing to protein aggregation (Sandelin *et al.* 2007). The glycine residue introduced in the D101G mutant protein may impart greater local flexibility to the protein structure than the asparagine in D101N (Betts & Russell 2003); and the greater flexibility around amino acid 101 when glycine is present could allow greater sampling of alternate conformations, promoting a shorter lag phase to aggregation. The D101N protein may also undergo deamidation potentially generating iso-aspartate at this position (Reissner & Aswad 2003). This alteration could have a negative influence on the nucleation of aggregates. Notably, cell-free translation studies of SOD1 maturation by Bruns et. al. observed a delay in the initial rate of the D101N mutant to fold (Bruns & Kopito 2007). The slower rate of folding would likely allow the protein to sample alternate conformations including conformations that allow self-assembly into aggregates. Although we do not fully understand how the different substitutions affect overall folding of mutant SOD1, both mutations produce a sufficient degree of instability to foster self-assembly into aggregates.

The major biophysical correlate to account for the distinct aggregation kinetics between the D101N and D101G mutants was the greater ability of the D101N mutant to acquire an intramolecular disulfide bond. Although significantly different ($p<0.05$) from WT SOD1, a far greater percentage of the D101N protein possessed a normal intramolecular disulfide bond than did the D101G mutant. This supports the previously mentioned Bruns et. al. study in which the formation of disulfide bonds was found to be identical for the D101N and WT SOD1 proteins in their cell-free translation system (Bruns & Kopito 2007). They also observed that other WT-like SOD1 mutant proteins such as the N134K and E100K variants efficiently acquired an intramolecular disulfide bond. We and others (Chattopadhyay *et al.* 2008, Furukawa et al. 2008, Jonsson *et al.* 2006, Karch et al. 2009) have previously noted that the fraction of mutant SOD1 that forms detergent-insoluble aggregates lacks an intramolecular disulfide bond. If the insoluble SOD1 aggregates are in fact produced from a fraction of the protein that lacks this modification (Karch et al. 2009), then it is possible that the slower rate of D101N aggregation is due to its greater efficiency in achieving an intramolecular disulfide bond. The more efficient formation of this modification would reduce the effective concentration of the precursor to aggregates, potentially leading to the longer lag phase to aggregate formation that we observe.

In our analysis of sensitivity of WT and mutant SOD1 to proteolytic digestion, we noted that whether reduced or oxidized, the D101N and D101G mutants in detergent-soluble fractions appeared more sensitive to digestion than WT SOD1 extracted in the same manner. However, we did note differences between the relative sensitivities of reduced and oxidized mutants to proteolysis as the oxidized fractions of both mutants retained some resistance to trypsin digestion. This finding indicates an important role of the disulfide bond in stabilizing the conformation of the SOD1 protein. For both mutants, the protein that partitioned into the detergent insoluble fractions displayed less resistance to trypsin degradation than either reduced or oxidized WT SOD1. Thus, in these aggregated mutant SOD1 proteins, significant regions of the protein are sufficiently disordered to allow access to trypsin digestion. It is notable that in this cell model, WT SOD1 is slow to aggregate and highly resistant to proteolysis even though a significant fraction of the protein fails to acquire the intramolecular disulfide bond. Thus, although post-translational modification of mutant SOD1 appears to be an important modulator of aggregation, WT SOD1 has evolved a sequence that inherently folds into a very stable structure even in the absence of stabilizing post-translational modifications.

The binding of metal cofactors to SOD1 contributes to the enzymatic activity and structural integrity of the protein (Chattopadhyay & Valentine 2009). Specifically, it has been demonstrated that WT SOD1 acquires resistance to protease digestion with the binding of Zn, not Cu (Bruns & Kopito 2007). Our findings agree with this prior study. Although the WT SOD1 protein was inefficient at binding Cu because of overexpression, the binding of Zn was about 1.5 atoms per dimer and both the reduced and oxidized forms of WT SOD1 were highly resistant to trypsin. In regard to the D101N and D101G mutants, both showed limited binding to both Cu and Zn and both mutants were highly sensitive to trypsin. Taken together, this data suggests that for the D101N and D101G mutants the binding of Zn may play a critical role in the acquisition of a conformation that resists proteolytic degradation.

In the present study we use a variety of biochemical techniques to further characterize the properties of the D101N and D101G SOD1 mutants that have been associated with fALS. While the D101N and D101G mutations are associated with fairly short disease durations of 2.5 years, previous studies have reported that the D101N mutant exhibits properties indistinguishable from the WT protein (Bystrom et al. 2010, Chattopadhyay & Valentine 2009, Rodriguez et al. 2005). However, in our overexpression model, we elaborate defects in D101N folding that include reduced efficiency of disulfide bond formation, high sensitivity to trypsin, and poor incorporation of zinc. Among these properties, D101N was very similar to D101G with the exception that the D101G mutant was significantly less efficient in forming the intramolecular disulfide bond. Additionally, we show that the different properties amounts of the D101N and D101G mutants that aggregate over 24 or 48 hour periods in our cell model is due to different rates of aggregate nucleation. Overall, our findings demonstrate that the D101N and D101G variants, which are both associated with relatively rapidly progressing disease, exhibit clearly distinctive features including different kinetics aggregation. Despite the general association between high aggregation propensity and disease duration (Prudencio et al. 2009b), the D101N variant seems to be a clear example of an exception to the rule and thus the biophysical characteristic of SOD1 that mediates rate of progression remains difficult to define.

Supplementary Material

Refer to Web version on PubMed Central for supplementary material.

Acknowledgments

This work was supported by a grant from the National Institutes of Neurological Disease and Stroke (P01 NS049134 – Program Project).

References

Betts, MJ.; Russell, RB. Amino acid properties and consequences of substitutions. In: Barnes, MR.; Gray, IC., editors. Bioinformatics for geneticists. Wiley; Hoboken, NJ: 2003. p. 289-316.

Borchelt DR, Guarnieri M, Wong PC, Lee MK, Slunt HS, Xu ZS, Sisodia SS, Price DL, Cleveland DW. Superoxide dismutase 1 subunits with mutations linked to familial amyotrophic lateral sclerosis do not affect wild-type subunit function. J Biol Chem. 1995; 270:3234–3238. [PubMed: 7852409]

Borchelt DR, Lee MK, Slunt HS, et al. Superoxide dismutase 1 with mutations linked to familial amyotrophic lateral sclerosis possesses significant activity. Proc Natl Acad Sci U S A. 1994; 91:8292–8296. [PubMed: 8058797]

Borchelt DR, Wong PC, Becher MW, et al. Axonal transport of mutant superoxide dismutase 1 and focal axonal abnormalities in the proximal axons of transgenic mice. Neurobiol Dis. 1998; 5:27–35. [PubMed: 9702785]

Bruijn LI, Houseweart MK, Kato S, Anderson KL, Anderson SD, Ohama E, Reaume AG, Scott RW, Cleveland DW. Aggregation and motor neuron toxicity of an ALS-linked SOD1 mutant independent from wild-type SOD1. Science. 1998; 281:1851–1854. [PubMed: 9743498]

Bruns CK, Kopito RR. Impaired post-translational folding of familial ALS-linked Cu, Zn superoxide dismutase mutants. EMBO J. 2007; 26:855–866. [PubMed: 17255946]

Bystrom R, Andersen PM, Grobner G, Oliveberg M. SOD1 mutations targeting surface hydrogen bonds promote amyotrophic lateral sclerosis without reducing apo-state stability. J Biol Chem. 2010; 285:19544–19552. [PubMed: 20189984]

Chattopadhyay M, Durazo A, Sohn SH, Strong CD, Gralla EB, Whitelegge JP, Valentine JS. Initiation and elongation in fibrillation of ALS-linked superoxide dismutase. Proc Natl Acad Sci U S A. 2008; 105:18663–18668. [PubMed: 19022905]

Chattopadhyay M, Valentine JS. Aggregation of copper-zinc superoxide dismutase in familial and sporadic ALS. Antioxid Redox Signal. 2009; 11:1603–1614. [PubMed: 19271992]

Cudkowicz ME, Warren L, Francis JW, Lloyd KJ, Friedlander RM, Borges LF, Kassem N, Munsat TL, Brown RH Jr. Intrathecal administration of recombinant human superoxide dismutase 1 in amyotrophic lateral sclerosis: a preliminary safety and pharmacokinetic study. Neurology. 1997; 49:213–222. [PubMed: 9222193]

Deng HX, Shi Y, Furukawa Y, et al. Conversion to the amyotrophic lateral sclerosis phenotype is associated with intermolecular linked insoluble aggregates of SOD1 in mitochondria. Proc Natl Acad Sci U S A. 2006; 103:7142–7147. [PubMed: 16636275]

Doucette PA, Whitson LJ, Cao X, Schirf V, Demeler B, Valentine JS, Hansen JC, Hart PJ. Dissociation of human copper-zinc superoxide dismutase dimers using chaotrope and reductant. Insights into the molecular basis for dimer stability. The Journal of biological chemistry. 2004; 279:54558–54566. [PubMed: 15485869]

Furukawa Y, Kaneko K, Yamanaka K, O'Halloran TV, Nukina N. Complete loss of post-translational modifications triggers fibrillar aggregation of SOD1 in the familial form of amyotrophic lateral sclerosis. The Journal of biological chemistry. 2008; 283:24167–24176. [PubMed: 18552350]

Jaarsma D, Haasdijk ED, Grashorn JA, Hawkins R, van Duijn W, Verspaget HW, London J, Holstege JC. Human Cu/Zn superoxide dismutase (SOD1) overexpression in mice causes mitochondrial vacuolization, axonal degeneration, and premature motoneuron death and accelerates motoneuron disease in mice expressing a familial amyotrophic lateral sclerosis mutant SOD1. Neurobiol Dis. 2000; 7:623–643. [PubMed: 11114261]

Jonsson PA, Graffmo KS, Andersen PM, Brannstrom T, Lindberg M, Oliveberg M, Marklund SL. Disulphide-reduced superoxide dismutase-1 in CNS of transgenic amyotrophic lateral sclerosis models. Brain. 2006; 129:451–464. [PubMed: 16330499]

Karch CM, Borchelt DR. A limited role for disulfide cross-linking in the aggregation of mutant SOD1 linked to familial amyotrophic lateral sclerosis. J Biol Chem. 2008; 283:13528–13537. [PubMed: 18316367]

Karch CM, Prudencio M, Winkler DD, Hart PJ, Borchelt DR. Role of mutant SOD1 disulfide oxidation and aggregation in the pathogenesis of familial ALS. Proc Natl Acad Sci U S A. 2009; 106:7774–7779. [PubMed: 19416874]

Lelie HL, Liba A, Bourassa MW, et al. Copper and zinc metallation status of copper-zinc superoxide dismutase from amyotrophic lateral sclerosis transgenic mice. J Biol Chem. 2011; 286:2795–2806. [PubMed: 21068388]

Potter SZ, Zhu H, Shaw BF, et al. Binding of a single zinc ion to one subunit of copper-zinc superoxide dismutase apoprotein substantially influences the structure and stability of the entire homodimeric protein. Journal of the American Chemical Society. 2007; 129:4575–4583. [PubMed: 17381088]

Prudencio M, Borchelt DR. Superoxide dismutase 1 encoding mutations linked to ALS adopts a spectrum of misfolded states. Mol Neurodegener. 2011; 6:77. [PubMed: 22094223]

Prudencio M, Durazo A, Whitelegge JP, Borchelt DR. Modulation of mutant superoxide dismutase 1 aggregation by co-expression of wild-type enzyme. J Neurochem. 2009a; 108:1009–1018. [PubMed: 19077113]

Prudencio M, Durazo A, Whitelegge JP, Borchelt DR. An examination of wild-type SOD1 in modulating the toxicity and aggregation of ALS-associated mutant SOD1. Hum Mol Genet. 2010; 19:4774–4789. [PubMed: 20871097]

Prudencio M, Hart PJ, Borchelt DR, Andersen PM. Variation in aggregation propensities among ALS-associated variants of SOD1: correlation to human disease. Hum Mol Genet. 2009b; 18:3217–3226. [PubMed: 19483195]

Prudencio M, Lelie H, Brown HH, Whitelegge JP, Valentine JS, Borchelt DR. A novel variant of human superoxide dismutase 1 harboring amyotrophic lateral sclerosis-associated and experimental mutations in metal-binding residues and free cysteines lacks toxicity in vivo. Journal of neurochemistry. 2012; 121:475–485. [PubMed: 22332887]

Ratovitski T, Corson LB, Strain J, Wong P, Cleveland DW, Culotta VC, Borchelt DR. Variation in the biochemical/biophysical properties of mutant superoxide dismutase 1 enzymes and the rate of disease progression in familial amyotrophic lateral sclerosis kindreds. Hum Mol Genet. 1999; 8:1451–1460. [PubMed: 10400992]

Reissner KJ, Aswad DW. Deamidation and isoaspartate formation in proteins: unwanted alterations or surreptitious signals? Cell Mol Life Sci. 2003; 60:1281–1295. [PubMed: 12943218]

Rodriguez JA, Shaw BF, Durazo A, et al. Destabilization of apoprotein is insufficient to explain Cu,Zn-superoxide dismutase-linked ALS pathogenesis. Proceedings of the National Academy of Sciences of the United States of America. 2005; 102:10516–10521. [PubMed: 16020530]

Sandelin E, Nordlund A, Andersen PM, Marklund SS, Oliveberg M. Amyotrophic lateral sclerosis-associated copper/zinc superoxide dismutase mutations preferentially reduce the repulsive charge of the proteins. J Biol Chem. 2007; 282:21230–21236. [PubMed: 17513298]

Wang J, Slunt H, Gonzales V, Fromholt D, Coonfield M, Copeland NG, Jenkins NA, Borchelt DR. Copper-binding-site-null SOD1 causes ALS in transgenic mice: aggregates of non-native SOD1 delineate a common feature. Hum Mol Genet. 2003; 12:2753–2764. [PubMed: 12966034]

Wang J, Xu G, Slunt HH, Gonzales V, Coonfield M, Fromholt D, Copeland NG, Jenkins NA, Borchelt DR. Coincident thresholds of mutant protein for paralytic disease and protein aggregation caused by restrictively expressed superoxide dismutase cDNA. Neurobiol Dis. 2005; 20:943–952. [PubMed: 16046140]

Watanabe M, Dykes-Hoberg M, Culotta VC, Price DL, Wong PC, Rothstein JD. Histological evidence of protein aggregation in mutant SOD1 transgenic mice and in amyotrophic lateral sclerosis neural tissues. Neurobiol Dis. 2001; 8:933–941. [PubMed: 11741389]

Zetterstrom P, Stewart HG, Bergemalm D, Jonsson PA, Graffmo KS, Andersen PM, Brannstrom T, Oliveberg M, Marklund SL. Soluble misfolded subfractions of mutant superoxide dismutase-1s are enriched in spinal cords throughout life in murine ALS models. Proceedings of the National Academy of Sciences of the United States of America. 2007; 104:14157–14162. [PubMed: 17715066]

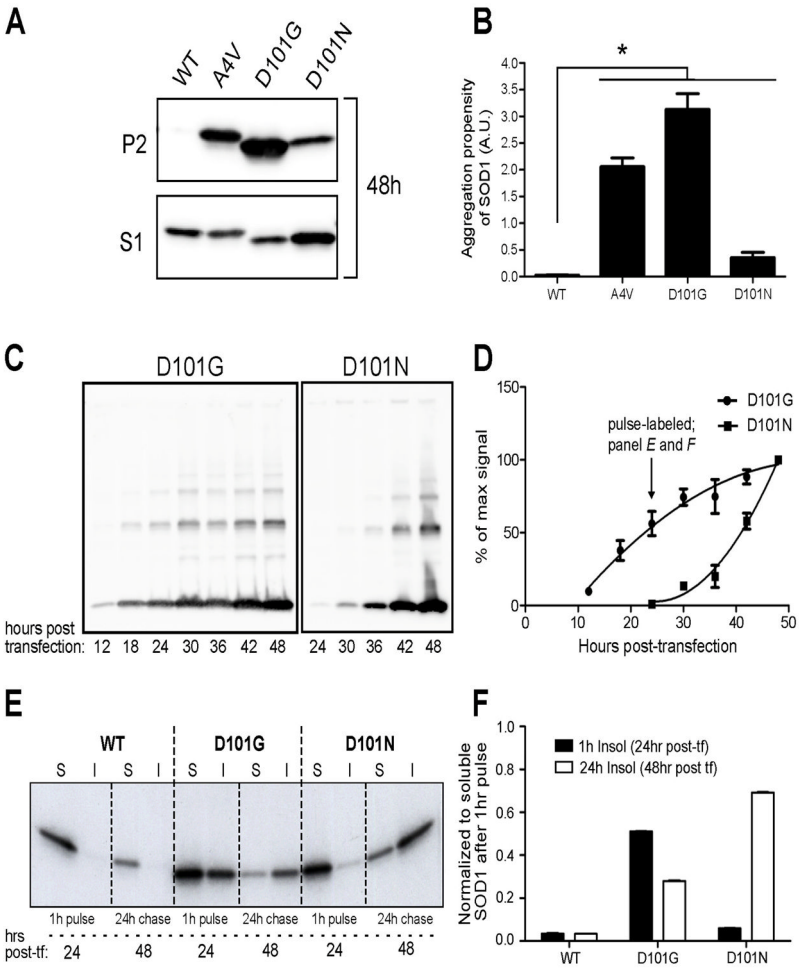

FIGURE 1.

Analysis of D101N and D101G variant aggregation. *A*, HEK293FT cells were transiently transfected with vectors to express WT or mutant hSOD1 for 48 hours before harvest and analysis of 5μg or 20μg of the NP-40 soluble (S1) or insoluble SOD1 (P2), respectively, by SDS-PAGE as described under "Methods". *B*, quantification of the aggregation propensity of the mutants analyzed in (A). Student's t-tests were performed to compare aggregation propensities of SOD1 proteins to WT SOD1, * $P \leq 0.05$, of three replicate experiments. *C*, transiently transfected HEK293FT cells expressing either D101G or D101N were collected at the indicated time-points post-transfection and 20μg of the NP-40 detergent insoluble SOD1 was analyzed by SDS-PAGE as described under "Methods". *D*, the band intensities at each time-point for D101G (circle) and D101N (square) were quantified in comparison to the intensity of the 48-hour signal (mean ratio ± S.E. (error bars) of three replicate experiments). A second order quadratic polynomial curve was fit for both mutants. To illustrate the relationship between the pulse-chase experiments and the overall aggregation time course, the 24hr time-point is highlighted as the point at which cells were metabolically radiolabeled. *E*, HEK293FT cells were transiently transfected (tf) with WT hSOD1 or mutant hSOD1 for 24 hours. Following radiolabeling of cells with ^{35}S Cys for one hour (1h), cells were either harvested or supplied with fresh unlabeled media for an additional 24 hours (24h) prior to harvesting. NP-40 soluble (S) and insoluble (I) fractions were then immunopurified and analyzed as described under "Methods". *F*, quantification of data illustrated in Panel *E*, comparing the amount of NP-40 insoluble protein formed in 1 or 24

hours for one construct in relation to its soluble fraction formed after 1 hour [mean ratio ± S.E. (error bars) of three replicate experiments]. An unpaired t-test was used to determine the statistical significance of the aggregation potential for each of the mutants when compared to wild type.

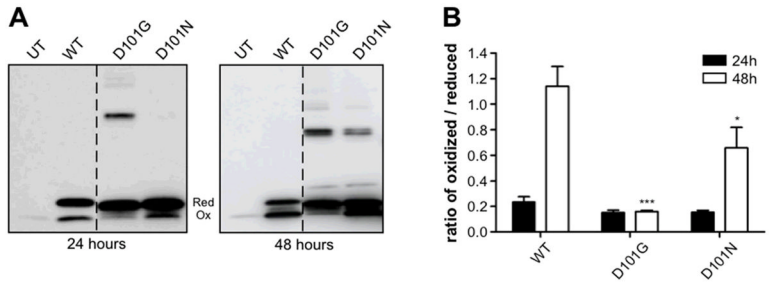

FIGURE 2.

Analysis of intramolecular disulfide bond formation by D101N and D101G variants of SOD1. Following transfection of HEK293FT cells for either 24 or 48 hours, as indicated, with WT SOD1, mutant SOD1 constructs, or left untransfected (UT), cells were detergent extracted in buffers containing iodoacetamide, as described under "Methods". *A*, 5μg of the detergent soluble fractions were analyzed by SDS-PAGE without reducing agent followed by an in-gel reduction in 2% β-mercaptoethanol. *B*, the ratio of oxidized (O) to reduced (R) SOD1 was quantified for each construct at both 24 and 48 hours [mean ratio ± S.E. (error bars) of three replicate experiments]. Analysis of variance (ANOVA) and Tukey's test was used to determine the statistical significance for each mutant SOD1 construct at either 24 or 48 hours when compared to WT at the same time point: * $P \leq 0.05$, ** $P \leq 0.01$, *** $P \leq 0.001$.

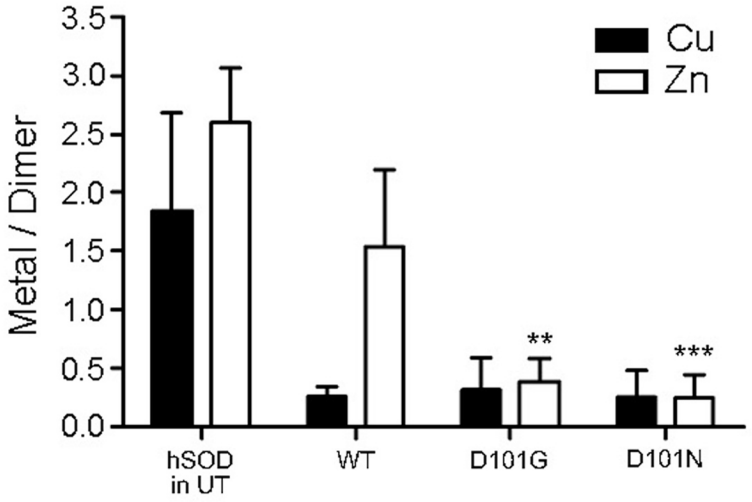

FIGURE 3.

Analysis of metal binding by D101N and D101G variants of SOD1. The copper (Cu) and zinc (Zn) metallation state of soluble human SOD1 from either untransfected HEK293FT cells or cells transfected for 24 hours with the SOD1 constructs listed were measured by HPLC-ICP-MS as described under “Methods”. The amount of Cu (black bars) and Zn (white bars) per dimer was calculated by dividing the metal concentration for each construct by its protein concentration [mean ratio ± S.E. (error bars) of at least three replicate experiments]. ANOVA and Tukey’s test was used to determine the statistical significance of the Cu and Zn levels for each of the mutants in comparison to the WT levels: ** $P \leq 0.01$, *** $P \leq 0.001$.

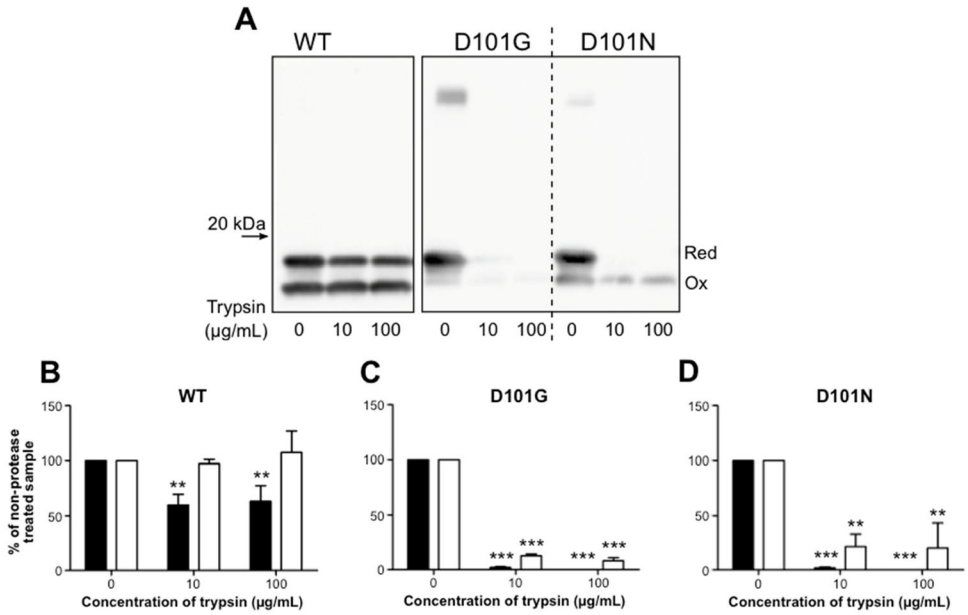

FIGURE 4.

Sensitivity of detergent-soluble forms of D101N and D101G SOD1 to proteolytic digestion. HEK293FT cells were transfected with the SOD1 constructs listed in panel *A* for 48 hours and detergent extracted in buffers containing iodoacetamide as described under “Methods”. *A*, 5μg of the NP-40 detergent soluble fractions were treated with varied concentrations of trypsin and analyzed by SDS-PAGE without reducing agent followed by an in-gel reduction in 2% β-mercaptoethanol. The migration of the 20kDa band of the ladder is indicated on the left of the panel. *B–D*, the reduced (black bars) and oxidized (white bars) band intensities for each SOD1 construct were quantified in relation to the non-trypsin treated fraction [mean ratio ± S.E. (error bars) of at least three replicate experiments]. ANOVA and Tukey’s test was used to determine the statistical significance of the band intensities for trypsin-treated reduced and oxidized SOD1 when compared to the non-treated samples: ** $P \leq 0.01$, *** $P \leq 0.001$. *Red*, reduced fraction; *Ox*, oxidized fraction.

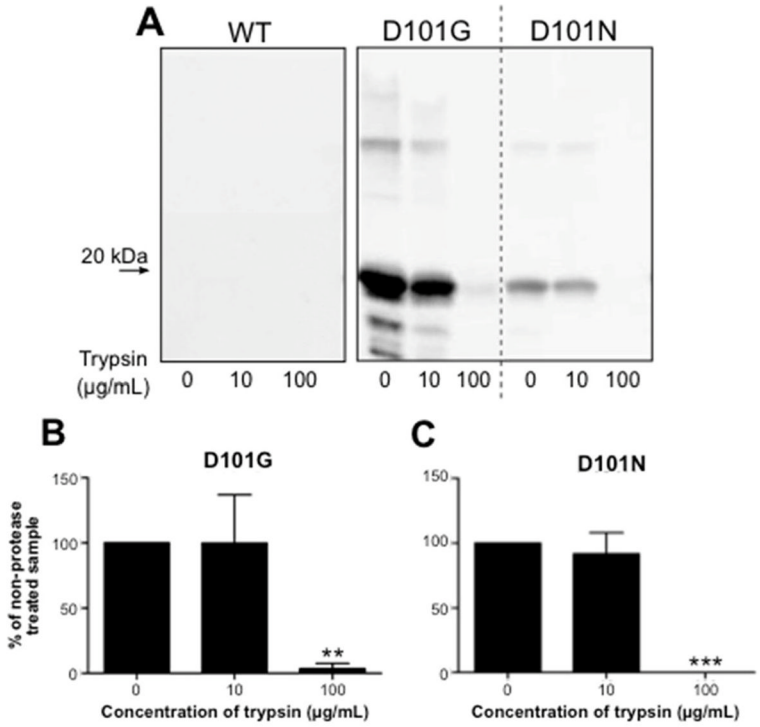

FIGURE 5.

Sensitivity of NP-40 insoluble forms of D101N and D101G SOD1 to proteolytic digestion. HEK293FT cells were transfected with the SOD1 constructs listed in panel *A* for 48 hours and detergent extracted in buffers containing iodoacetamide as described under “Methods”. *A*, 20μg of the NP-40 detergent insoluble fractions were treated with varied concentrations of trypsin and analyzed by SDS-PAGE. The migration of the 20kDa band of the ladder is indicated on the left of the panel. *B–D*, the intensity of the band representing monomer SOD1 (~16kDa or most intense band) for each SOD1 construct was quantified in relation to the non-trypsin treated fraction [mean ratio ± S.E. (error bars) of three replicate experiments]. ANOVA and Tukey’s test was used to determine the statistical significance of the trypsin treated band intensities when compared to the non-treated samples: ** $P \leq 0.01$, *** $P \leq 0.001$.

Table 1

Comparison of SOD1 properties

Variant	Disease Duration[a]	Aggregation propensity at 48h	Ratio of Oxidized to Reduced	Trypsin Resistant (100ug/mL) - Soluble		Trypsin Resistant –Insoluble		Zn bound per dimer
				Reduced	Oxidized	10 ug/ml	100ug/ml	
WT	NA[a]	Low	0.90	63%	108%	NA	NA	1.5
D101G	2.5 yr	Extreme	0.19	0%	8%	100%	4%	0.4
D101N	2.4 yr	Low	0.48	0%	20%	92%	0%	0.2

[a]Not applicable